Optimisation dynamique de l'empreinte carbone et de l'efficacité énergétique d'un site de production de pétrole offshore : Une approche intégrée exergétique

Optimizing the carbon footprint of an offshore upstream asset by maximizing its energy efficiency : An integrated exergetic modelling approach

Nathan SENECHAU[12*], Maxime HIGELIN[1], Laurent AVAULLEE[1], Sylvain SERRA[2], Sabine SOCHARD[2], Jean-Michel RENEAUME[2]

[1] TotalEnergies SE, Pau, France
[2] Universite de Pau et des Pays de l'Adour, LaTEP, Pau, France
* (nathan.senechau@univ-pau.fr)

Résumé - L'objectif de cette étude consiste à proposer une nouvelle méthodologie pour la modélisation et l'optimisation dynamique exergétique des sites offshore pétroliers intégrant l'ensemble de la chaine fluide. Cette nouvelle méthodologie a été appliquée à un champ offshore à taille réelle exploité par la Compagnie TotalEnergies au large de l'Angola appelé 'Girassol'. Ce modèle est utilisé afin de comparer l'optimisation dynamique respectivement des irréversibilités et de l'empreinte carbone du site en vue de réduire ses émissions et d'améliorer son rendement énergétique sur l'ensemble de sa durée de vie.

Abstract - The objective of this study is to propose a new methodology for the dynamic exergy-based modelling and optimization of offshore oil sites, integrating the entire fluid chain. This novel approach is developed using a full-scale offshore field operated by TotalEnergies off the coast of Angola, known as 'Girassol'. The model applies dynamical optimization to compare both the irreversibilities and the site's carbon footprint, with the aim of reducing its emissions and improving its energy efficiency.

Nomenclature

b Molar exergy, $\mathrm{J/mol}$
C_{oil} Standard cumulated oil rate, STB
g Gravitational acceleration constant, $\mathrm{m/s^2}$
Δh Molar enthalpy deviation, $\mathrm{J/mol}$
$\dot{I}$ Irreversibilities, $\mathrm{J/s}$
IP Well productivity index, $\mathrm{STB/(bara \cdot s)}$
N, Nc Total number of timestep and component
$\dot{n}$ Molar flowrate, $\mathrm{mol/s}$
P Pressure, bara
ΔP Deviation from atmospheric pressure, bara
R Ideal gas constant, $\mathrm{J/mol \cdot K}$
Δs Molar entropy deviation, $\mathrm{J/mol \cdot K}$
t Time, s
T Temperature, K
ΔT Deviation from ambient temperature, K
$\dot{V}$ Standard volumetric rate, $\mathrm{STB/d}$
$\dot{W}$ Mechanical or electrical work, W
z_a Altitude, m
z Molar composition fraction

Symboles grecs

ϕ Fugacity coefficient
τ Time horizon period

Indices et exposants

bhp Bottom well pressure
ie, is, j Inlet, outlet stream, work source
k, q Chemical, simple pure component
lin Res to bottom well liquid rate
$lout$ Bottom to head well liquid rate
o, g, w Oil, gas, water
res Reservoir
whp Well head pressure
$*$ Ideal gas state
$_0$ Ambiant conditions

https://doi.org/10.25855/SFT2026-024

1. Introduction

1.1. Context

TotalEnergies operates several offshore oil and gas production plants off the coast of Angola. In particular, the oldest Floating Production Storage and Offloading (FPSO) unit still in operation on a deep offshore field is the Girassol FPSO. In recent years, monitoring of greenhouse gas (GHG) emissions has shown that more than 60% of the GHG emissions from the company's offshore oil and gas production assets result from the combustion of fuel gas in the gas turbines [1], which supply the FPSO with electrical power, totaling around 60 to 75 MWelec.

1.2. Objectives

Exergetic theory has been fully developed, tested, and used since the beginning of the 20th century in a wide range of industrial sectors, including oil and gas [2]. Its ability to assist engineers in retrofitting and operational optimization of industrial systems has already been demonstrated. In the case of offshore oil and gas plants, exergetic analysis has been applied separately to both the subsurface and surface areas in few relevant works [3]-[7]. However, the design of offshore assets highly depends on the site conditions consequently the modelling and optimization results are very specific to the site [8]-[11]. None of these studies have taken into account the fact that on FPSOs, there are material and energetic feedback mechanisms such as gas-lift and water flow rates toward the subsurface, which are critical to better understanding the behavior of these installations and improving their energy efficiency and CO_2 emissions. Therefore, this is the novelty of this work, we implement exergy computation in a dynamic, integrated offshore FPSO model and dynamically optimized operational variables with an ojective function constituted with irreversibilities or carbon footprint. The surface process of the FPSO mainly consists of the separation train, the recompression train, the gas turbines, and water treatment and reinjection. The separation train is composed of three separation stages (HP high, MP middle, and LP low pressure separators). The flowsheet structure of the Girassol offshore field is presented in Figure 1 below :

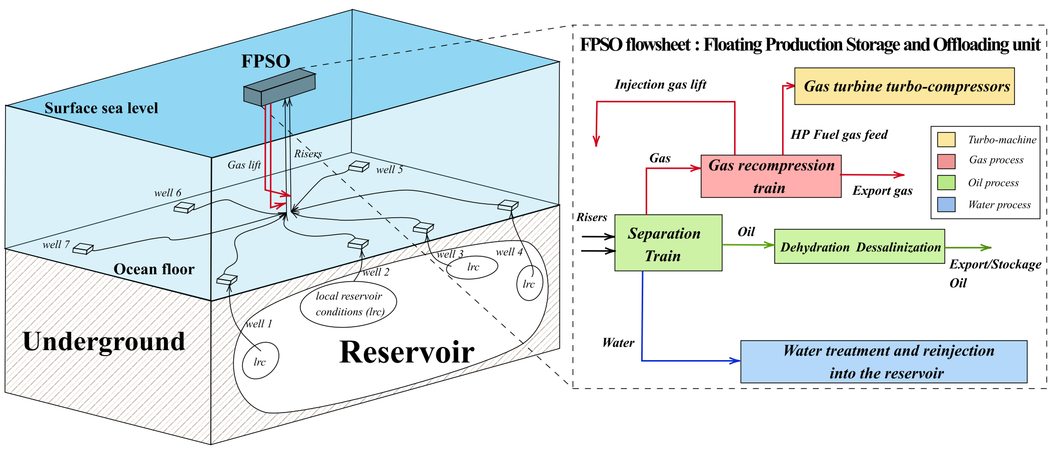

Figure 1 : *Girassol field flowsheet*

2. Methodology and tools

2.1. Exergy computation methodology

The exergy is computed in this work using the homogeneous thermodynamic approach [12] considering that kinetic exergy is negligible. In this method, exergy is defined by the following equation [13]-[15] :

$$b = \Delta h(\Delta T, \Delta P, z) - T_0 \Delta s(\Delta T, \Delta P, z) + \sum_{i=k}^{N_c} z_k [b_k^{0,*} + RT_0 ln(z_k \phi_k)] + g z_a \quad (1)$$

The molar exergy b is defined as a function of enthalpy deviation Δh and entropy deviation Δs. The reference enthalpy is the ideal gas enthalpy of formation at 1 bar and 298 K, defined as zero, $\Delta T = T - T_0$, $\Delta P = P - P_0$. The chemical exergy is computed by the standard ideal gas exergy $b_k^{0,*}$ introduced by Szargut et al in 1989 [16], [17] where each k component is a combination of different q pure simple components according to a ν_q stoichiometric formation coefficient. Then at each monthly time step the exergy losses are included in the exergy destruction [15]. In our study we will consider that at each monthly time step t our system is in steady state as simulation dynamics are governed exclusively by the monthly evolution of reservoir conditions associated with its depletion through the time. The exergetic balance on the system can be expressed by the following equation :

$$\sum_j \dot{W}_j + \sum_i \dot{n}_{i,e} b_{i,e} - \dot{n}_{i,s} b_{i,s} - \dot{I} = 0 \quad (2)$$

This exergetic method has been implemented in C++ in the software BEST [18], developed by the Company for thermodynamic simulation purposes.

2.2. Surface model

The BEST software uses a homogeneous approach with equations of state (EoS) to compute enthalpy and entropy of the stream; in our case, the Peng-Robinson equation of 1978 with the modification by Soreid & Whitson (1992) for water-hydrocarbon interactions is used. BEST is able to perform phase equilibrium calculations, such as multiple flash calculations, as well as polytropic compression, pumping, and expansion turbine simulations. Gas turbine power production is necessary to supply in electricity and mechanical work the compressors and pumps that handle gas recompression and water reinjection into the reservoir. The power-consuming equipment includes the electrical gas compressors from the LP and MP stages, recycling oil and water pumps, cooling loop and raw seawater pumps. Six turbo-compressors are used for the HP compression train supplied by two turbines drivers. The last type of equipment are the two water reinjection pumps, each with its own driver turbine. For gas turbine modelling, it was necessary to implement the model in pure Python because none of the softwares proposed in this study could have correctly simulated the gas turbines present on the Girassol FPSO, especially with a model that takes into account the engine supplier curve. Data from these curves enable us to compute the realistic operating point of the turbines based on certain functional parameters. These parameters include the ambient air temperature entering the compressor and the net power required from the turbine to supply in electricity other equipments. The continuous extrapolation toward zero is handled by Bezier curves [19], allowing the optimizer to eventually converge to a state in which one of the turbine is off and the second is at partial load.

2.3. Subsurface model

The modelling of the subsurface equipment flowsheet has been done with the software GAP from the IPM Petroleum Engineer Expert PETEX software solution [20]. This tool is used by the Company to simulate the properties and the amount of each phase flowrate from the bottom of the wells to the top of the network thanks to the Black-Oil (BO) method. Girassol field is composed of three main reservoirs but in the BO model each well corresponds to a dataset of local reservoir conditions as shown in Figure 1. We detail below this method just for one well at a time step t. First GAP applies linear interpolation using the well and reservoir dataset to determine the reservoir pressure P_{res} and the well bottom conditions : the well's productivity index IP (which depends on the geometry parameters of the completion and the mechanical properties of the fluid), the oil/gas ratio GOR, and the water/liquid ratio WCT depending on the cumulative oil production $C_{oil}(t)$. Then GAP computes the flowrate between the reservoir and the bottom of the well $\dot{V}_{lin}$ expressed as a function of IP and the difference between the reservoir pressure P_{res} and the bottom hole pressure P_{bhp} : $\dot{V}_{lin} = IP(P_{res} - P_{bhp})$. Secondly GAP computes a dataset of the flowrate through the well, $\dot{V}_{lout}$, for various ranges of P_{whp} well head pressure. The correct liquid volumetric rate is deduced from the intersection between the $\dot{V}_{lin}$ and the corresponding $\dot{V}_{lout}$ curve cf Figure 2. The $\dot{V}_o$ oil volumetric rate determined is add to the last cumulated oil production $C_{oil}(t)$ and then this new cumulated oil value $C_{oil}(t+dt)$ is used to compute the new bottom well conditions. GAP releases this loop for each well. Once all the wells flowrates have been computed, GAP resolves the network mass and energy balances by using pressure loss correlations. Pipe's temperatures are computed independently by a thermal equation with no spatial dependency and a constant heat loss transfer coefficient depending on the pipe material and the surrounding temperature of the wall. This temperature is determined from an Angola sea water temperature dataset as a function of depth.

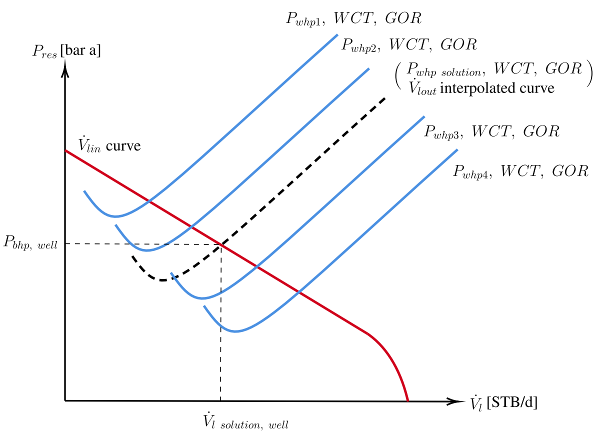

Figure 2 : $\dot{V}_{lin}$ / $\dot{V}_{lout}$ *intersection*

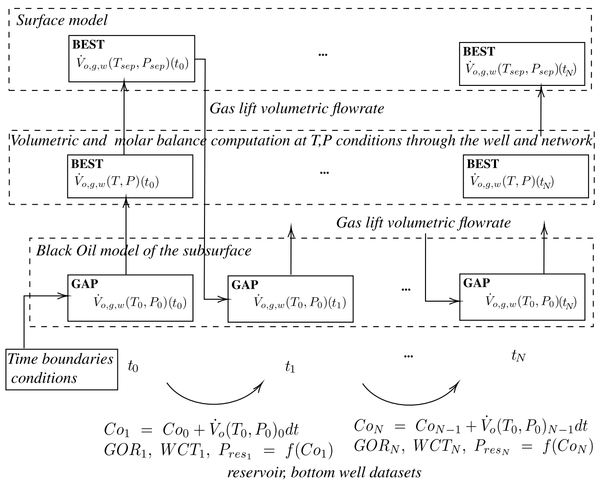

Figure 3 : *Workflow GAP/BEST*

2.4. Python coupling model

The coupling between the two software packages involves on the one hand utilizing the BEST software, which enables exergy calculations and surface process simulation and on the other hand using GAP for the subsurface with the PETEX 'Open Server' API [20]. At the beginning it is necessary to initialize the reservoirs with the corresponding historical cumulative production data as shown on the Figure 3. If the simulation starts after the historical start date of gas lift operations, it is also necessary to initialize the density and molar composition of the gas lift in GAP. Once initialization is complete, allocation and flow rates of gas lift between risers can be set, subject to the maximum gas lift flow rate constraint. The GAP solver is then called to resolve the entire subsurface model and determine pressures, temperatures, and standard volumetric flow rates of oil, gas, and water at each node of the subsurface network, from the reservoirs to the inlet of the first surface three-phase separator cf 2.3. The BEST software then performs a mirror simulation of the GAP subsurface model to calculate the molar compositions corresponding to the standard flow rates at each node. A sequence of pressure and temperature flashes enables calculation of the respective thermodynamic states at the bottomhole, wellhead, and gas lift injection nodes in the network. BEST then carries out the material balance for the surface model before calculating energy balances to determine surface mechanical and electrical power requirements. Finally, the gas turbine models are called to cover the site's power balance. Ultimately, BEST executes an exergy balance for the entire petroleum production chain. The dynamic simulation integrates the execution of this sequential loop until the simulation time horizon of 23 years is reached.

3. Results and discussions

3.1. Model validation

In the integrated surface-subsurface model, the volumetric balance between the simulation and historical data is validated over the entire field lifespan on the Figure 4, with an **absolute error** around **10%** on model prediction for oil and gas rate. However the error on the water rate increase to **5** $\sim$ **15 %** with the time. This error is due to the lack of accuracy of the IP historical dataset used by the BO model from GAP to interpolate the IP of each well at each time step. It will be necessary to fix the historical data of IP and perform again the simulation to reach better result on the water rate. Nevertheless, the impact of this discrepancies on the water rate is not a problem for the optimization studies that will follow in this work. The model

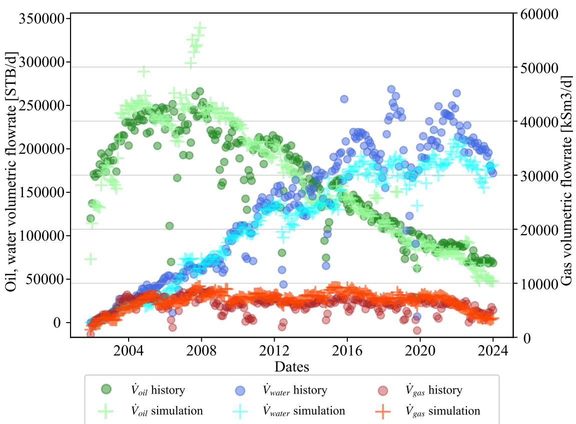

Figure 4 : *Oil, gas & water production history match*

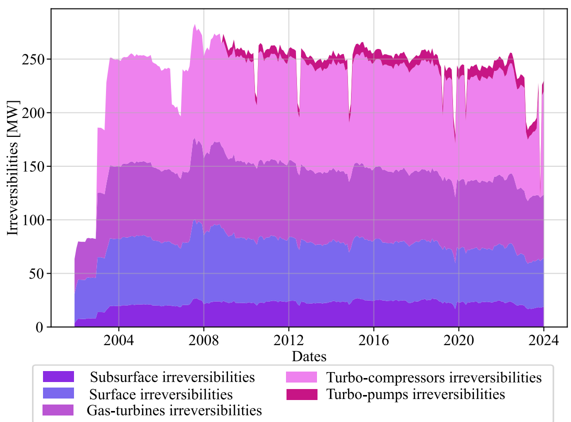

Figure 5 : *Irreversibilities simulation*

estimates that over **80% of the irreversibilities comes from the surface equipment** as suggest in Figure 5. This first result hopefully shows that it is possible to optimize the entire site carbon footprint and irreversibilities by changing the operational variables like process variables in the gas turbine for instance.

3.2. Separation pressure sensitivity analysis

In our case study, the operational variables that can be concretely adjusted at the surface level are the separation and the recompression pressures and the allocation of load rates among the turbogenerators.This section provides a detailed sensitivity analysis of the high-pressure separation pressure in the first three-phase separator at the surface processing facilities. The operating pressure of this separator has a significant impact on overall oil production, energy consumption, and carbon footprint. The sensitivity analysis was carried out over the course of a year after the peak production of the field (2007/2008), with a time step of one month and pressure discretization over four months. The graph in Figure 6 enables identification of the variations

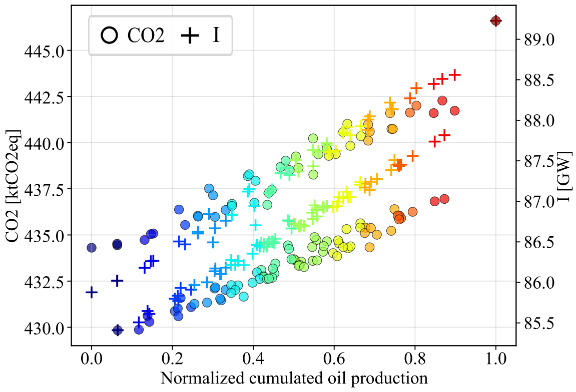

Figure 6 : *CO_2/I influence pressure*

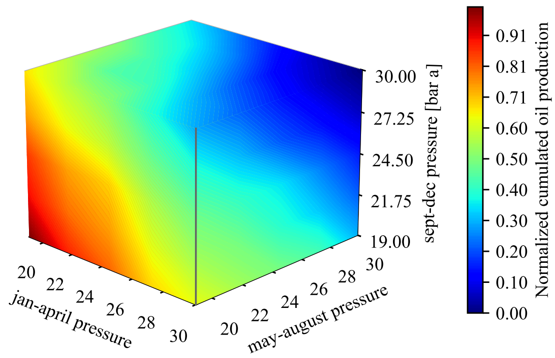

Figure 7 : *Cumulated oil influence pressure*

of the CO_2 emissions from the site on the left-hand y-axis and irreversibilities on the right-hand y-axis as a function of the normalized cumulative oil production as it is confidential data. The colour schemes of the graphs in the Figures 6 and 7 are equivalent. Figure 7 shows the response surface of variations in cumulative oil production directly in relation to the temporal variations of the surface HP separator pressure. Sensitivity analysis of the first high-pressure surface separator demonstrates the **direct dynamic correlation between CO_2 emissions and offshore site irreversibilities**. The sensitivity analysis demonstrate the **linear influence** of the **separation pressure** on both CO_2 emissions and irreversibilities of the site. The Figure 6 suggest that there is optimal range of separation pressure for reducing CO_2 emissions and irreversibilities under the same oil production constraint. An **increase of 7 % of the oil production corresponds to an increase of 2.5 % of the CO_2 emissions and 3.5 % of the irreversibilities**. Thus it is more relevant to optimize the carbon footprint/irreversibilities intensity of the field production to find the optimal separation pressure solutions compared to the historical constant pressure of 25 bar to reduce CO_2 emissions and irreversibilities while improving oil production of the site.

3.3. Gas turbines load allocation optimization

Another interesting variable for optimization is the gas turbine load. The power required to supply the surface process is generally above 25 MW for most of the field's lifespan, so both gas turbines are always running. This configuration allows us to optimize power distribution between the two turbines over time. This dynamic optimization problem is defined as follows :

$$\underset{l_1,l_2}{\text{Min}}\ \mathcal{I} = \int_0^{\tau} \dot{I}(l_{1,2}(t))\,dt \quad \text{or} \quad \underset{l_1,l_2}{\text{Min}}\ \mathcal{CO}_2 = \int_0^{\tau} \dot{CO}_2(l_{1,2}(t))\,dt$$

$$\forall t \in [0,\tau] \qquad l_1(t)\dot{W}_{\max}(T_0(t)) + l_2(t)\dot{W}_{\max}(T_0(t)) - \dot{W}_{GT}(t) = 0 \tag{3}$$

$$l_1 - l_2 > 0 \tag{4}$$

$$0 \leq l_{1,2} \leq 1 \tag{5}$$

The equality constraint (3) define that the sum of the power called at each gas turbine $l_1\dot{W}_{\max}$; $l_2\dot{W}_{\max}$ where $\dot{W}_{\max}$ is the maximum work callable at the ambiant air temperature T_0 at the timestep t has to be equal to the power need $\dot{W}_{GT}(t)$ of the process equipment. The boundary conditions on the turbine load are defined by inequality (5). Inequality (4) expresses the symmetry of the problem, as the values of l_1 and l_2 are interchangeable. CO_2 emissions and I are equivalent for the solution $l_1 = 1; l_2 = 0$ and $l_1 = 0; l_2 = 1$ positions in the domain of research. The optimization solutions are shown in Figures 8 and 9 for both the CO_2 emissions

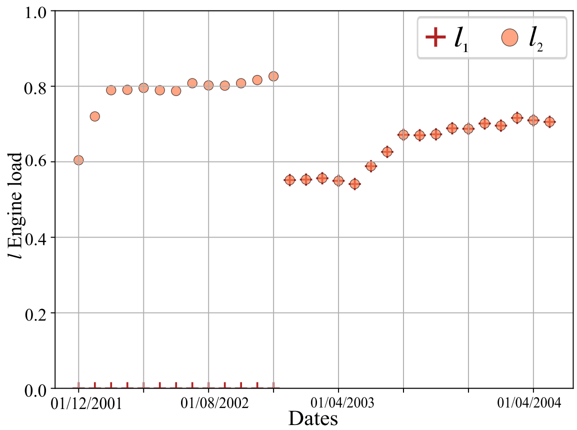

Figure 8 : CO_2 *optimization results*

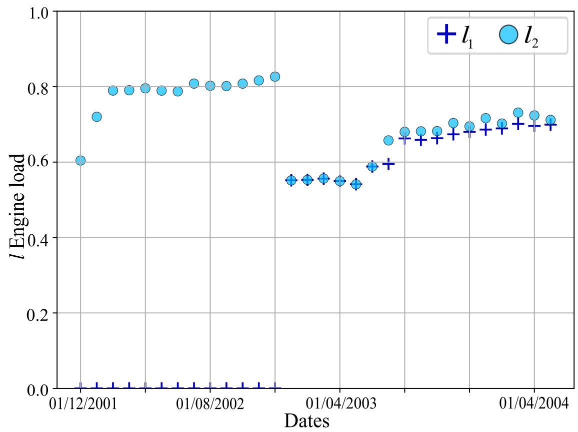

Figure 9 : $\dot{I}$ *optimization results*

and I irreversibility objective functions. As the model is a black-box nonlinear function under linear certain constraints (3), the 'SLSQP' algorithm of the scipy library has been used to solve this optimization problem [21]. The gas turbine optimization shows that it is preferable to use a single turbine at full load as long as possible, then to **distribute power equally between the turbines to minimize CO_2 and irreversibilities**, which confirms results in the literature regarding minimization of the entropy generation in complex systems [22],[23].

4. Conclusions and perspectives

This study has demonstrated that irreversibilities as an objective function, can substitute for CO_2 emissions in terms of the optimisation variables on which the offshore oil and gas production system depends. Exergy is an analytical function that can be calculated only from pressure, temperature, and chemical composition data. It could therefore replace CO_2 emissions as an indicator when these are too complex to monitor or when supplier's performance curves for gas turbines are unavailable. Furthermore, this objective function enables the integration of both an energy performance and a greenhouse gas emissions criteria into a single objective function. Indeed, a reduction in irreversibilities corresponds to a decrease in CO_2 emissions and an improvement in the system's energy efficiency, as less work is required to produce the same amount of energy in the form of oil. Finally the work forward of this study will be focused on resolution of both high-pressure separation and gas lift risers allocation dynamic optimization problem over the entire lifetime of the field to search for non linearity and then find optimum with lower CO_2 emissions and irreversibilities under cumulated oil and gas production constraint.

References

[1] TotalEnergies, Sustainability and Climate Progress Report, (2025).

[2] E.Sciubba, G.Wall, *A brief Commented History of Exergy From the beginnings to 2004*, Journal of Thermodynamics, 10-1 (2007), 1-26.

[3] M.Akchiche, *Analyse exergétique et optimisation dynamique des systèmes de production d'hydrocarbures dans la perspective de réduire les émissions de CO_2*, Université de Pau et des pays de l'Adour, (2020)

[4] T.V.Nguyen, T.Jacyno, P.Breuhaus, M.Voldsund, B.Elmegaard, *Thermodynamic analysis of an upstream petroleum plant operated on a mature field.*, Energy, 68 (2014), 464-469.

[5] S. de Oliveira Jr, M. Von Hombeeck, *Exergy analysis of Petroleum separation processes in offshore platforms*, Energy convers, Institute for Technological Research and Polytechnic School of the University of Sao Paulo, 38-15 (1997), 1577-1584.

[6] J.A.M.da Silva, S. de Oliveira Jr, *Unit exergy cost and CO_2 emissions of offshore petroleum production*, Energy, 147 (2018), 757-766.

[7] T.V.Nguyen, L.Pierobon, B.Elmegaard, F.Haglind, P.Breuhaus, M.Voldsund, *Exergetic assessment of energy systems on North Sea oil and gas platforms*, Energy, 62 (2013), 23-36.

[8] M.Voldsund, T.V.Nguyen, B.Elmegaard, I.S.Ertesvåg, A.Røsjorde, K.Jøssang, S.Kjelstrup, *Exergy destruction and losses on four North Sea offshore platforms : A comparative study of the oil and gas processing plants.*, Energy, 74 (2014), 45–58

[9] T.V.Nguyen ; M.Voldsund ; B.Elmegaard ; I.S.Ertesvåg ; S.Kjelstrup, *On the definition of exergy efficiencies for petroleum systems : Application to offshore oil and gas processing*, Energy, 73 (2014), 264-281

[10] T.V.Nguyen, T.G.Fülöp, P.Breuhaus, B.Elmegaard, *Life performance of oil and gas platforms : site integration and thermodynamic evaluation*, Energy, 73 (2014), 282-301

[11] M.Voldsund, T.V.Nguyen, B.Elmegaard, I.S.Ertesvåg, S.Kjelstrup, *Thermodynamic performance indicators for evaluation of North Sea oil and gas platforms*, Journal of Oil and Gas facilities, 3 (2014), 51-63.

[12] S.Gourmelon, *Méthodologie d'analyse et de rétro-conception pour l'amélioration énergétique des procédés industriels*, INP Toulouse, (2015)

[13] R.Benelmir, A.Lallemand, M.Feidt, *Analyse exergétique, Définitions*, Energies — Physique énergétique (2002).

[14] A.Lallemand, *Thermodynamique appliquée-Bilans entropiques et exergétiques*, Énergies — Physique énergétique (2021).

[15] R.Benelmir, *Analyse exergétique - Applications*, Energies — Physique énergétique (2019).

[16] J.Szargut, *Chemical exergy of the Elements*, Applied energy, 32 (1989), 269-286

[17] R.Rivero, M.Garfias, *Standard chemical exergy of elements updated*, Energy, 31 (2006).

[18] BEST Basic Element for Simulation in Thermodynamic, BEST TotalEnergies's software, v13.0,(2025)

[19] E.Rahmanovic, M.Petrun, *Analysis of Higher-Order Bézier Curves for Approximation of the Static Magnetic Properties of NO Electrical Steels*, Mathematics, 12, (2024), 445.

[20] PETEX Petroleum Experts Limited, IPM GAP Multiphase Flow Production Optimiser, v14.0,(2022)

[21] Lawson, C. L., and R. J. Hanson, *Solving Least Squares Problems*, SIAM, Philadelphia, PA, (1995).

[22] B.Kilkis, *Is exergy destruction minimization the same thing as energy efficiency maximization ?*, Journal of Energy Systems, (2021), 165-184.

[23] A.Bejan, *Entropy generation minimization : The new thermodynamics of finite-size devices and finite-time processes*, Journal of Applied Physics, 79 (1995).